Electrically conductive hydrogels with controlled drug release for cartilage tissue engineering

Filipe Alexandre Rodrigues Miguel

Master in Biotechnology

Articular cartilage is a highly specialized tissue, adapted to bear significant compressive loads in diarthrodial joints, being crucial for healthy articular motion. However, the absence of vascularization, low chondrocyte density and low proliferative potential inhibit an effective self-healing of the tissue after lesions or degeneration. Osteoarthritis, which results in the progressive degeneration of cartilage, is the most prevalent joint disorder, being a major cause of pain and disability worldwide. The most common treatment options for this condition are primarily focused on pain relief, failing to address tissue regeneration. Cartilage tissue engineering (CTE) focuses on the development of cartilage constructs through the combination of biomaterials with cells and bioactive factors (biochemical and physical). The potential of CTE to create engineered tissues with structural, mechanical, and functional properties similar to the native articular cartilage makes it a promising alternative to the current clinical approaches for cartilage repair. Hydrogels appeared as a suitable candidate for CTE due to their ability to recapitulate the biophysical properties of native cartilage. Moreover, hydrogels can be combined with conductive materials to mimic the natural electrochemical features of articular cartilage. Thus, in this work, electrically conductive hydrogels composed by hyaluronic acid-chondroitin sulfate and PEDOT nanoparticles were synthesized and characterized in terms of their structural, rheological and electrical properties. The nanoparticles were loaded with a chondro-inductive drug, kartogenin, and characterized in terms of morphology, size, surface charge, biocompatibility and drug release kinetics. Kartogenin release was shown to be tightly controlled by external electrical stimulation. Kartogenin-loaded PEDOT nanoparticles were incorporated in hydrogels together with human mesenchymal stem/stromal cells (MSCs) and exposed to electrical stimulation. Finally, the ability of the hydrogel system to promote the chondrogenic differentiation of MSCs was also assessed. Overall, the controlled release of the drug was demonstrated, and the proposed system exhibited promising results in promoting the proliferation and chondrogenic differentiation of MSCs, highlighting its potential for CTE applications.

Keywords: Cartilage tissue engineering, Drug delivery systems, Hydrogels, Kartogenin/PEDOT nanoparticles, Mesenchymal stem/stromal cells

1. Introduction

Articular cartilage is a highly complex and specialized connective tissue present in diarthrodial joints, being paramount for healthy joint mobility. The tissue is able to provide a smooth and highly durable surface that facilitates the transmission of mechanical loads with a low friction index. It comprises a single cell type (chondrocytes), which are embedded in a dense matrix composed by collagen type II and proteoglycans, with glycosaminoglycans (GAGs) as side chains[1]. This tissue has a multilayered structure encompassing high quantities of water retained within the matrix pores and intrafibrillar space[2]. When experiencing mechanical stress, the water is able to flow through the matrix of the tissue, and it is the high frictional resistance to this flow that allows articular cartilage to withstand such high mechanical loads. Despite its importance for healthy motion, the avascularity of this tissue severely limits its self-healing capacities upon lesions or degeneration. This problem is further exacerbated by the prominence of degenerative cartilage conditions like osteoarthritis (OA). OA is the most common joint disorder, characterized by severe pain and loss of mobility as result of the progressive loss of articular cartilage, thickening of the subchondral plate and development of cysts in the subchondral bone[3]. It is estimated that

360 million people are currently affected by OA, with knee OA affecting approximately 10% of men and 13% of women over 60 years old, while hip OA affects 6,1% of men and 13% of women over 65 years[4–6]. Additionally, as key predicators, the number of people affected by OA is estimated to keep increasing as a consequence of the obesity epidemic and population aging, with data suggesting an additional 26 thousand adults per 1 million will experience OA by 2032[7]. Despite its prevalence and socioeconomic impact, the pathogenesis of OA remains largely unknown, and the current non-arthroplasty treatments only offer short-term solutions, failing to rectify the core pathophysiological mechanisms that underly the degeneration of cartilage. Considering the unmet medical needs for the effective treatment of OA, cartilage tissue engineering (CTE) has emerged as a promising alternative to treat cartilage defects[8]. CTE employs the use of a biocompatible, biodegradable and biomimetic biomaterial scaffolds that are combined with cells (chondrocytes or stem cells) and bioactive factors (e.g., growth factors, physical stimuli) to promote cell proliferation, differentiation and maturation, ultimately leading to tissue regeneration[9]. In this project, kartogenin (KTG), a chondrogenic inducing small molecule, was loaded into poly(3,4-ethylenedioxythiophene) (PEDOT) nanoparticles (NPs), which were then embedded in an electrically conductive hyaluronic acid-PEGDA-chondroitin sulfate hydrogel (HA-CS). The nanoparticles were characterized in terms of their size, stability, and electrochemical properties. The hydrogel scaffolds were characterized in terms of their morphological and biophysical/chemical (e.g., rheology, swelling, water uptake, electrical conductivity) properties. *In vitro* cell culture assays were performed to optimize both the concentration of PEDOT NPS/KTG to use and the electrical stimulation protocol for controlled KTG release. The potential of electrical stimuli-controlled KTG release in promoting the chondrogenic differentiation of mesenchymal stem cells (MSCs) was first assessed in 2D monolayer cultures. Finally, the conductive hydrogels were combined with MSCs, and their potential to induce chondrogenic differentiation by kartogenin release through external electrical stimulation was also assessed.

2. Materials and methods

2.1 PEDOT and KTG/PEDOT nanoparticles fabrication

PEDOT and KTG-loaded PEDOT NPs were produced through in situ emulsion polymerization. A detergent, sodium dodecyl benzenesulfonate (DBSA, Sigma Aldrich), was added to miliQ water at 9.3 mM and magnetically stirred (750 rpm) at 40ºC in a hot plate (RCT Classic; IKA) for 1 hour in order to form micelles. 3,4-Ethylenedioxythiophene (EDOT) (Sigma Aldrich) was added to the solution to a final concentration of 32.2 mM and, in the case of KTG-loaded NPs, a 4mg/ml KTG in DMSO solution was also added to the mixture for a final concentration of 0.4 mg/ml, which was then magnetically stirred (750 rpm) at 40ºC for 1 hour. Finally, a 182,4 mg/ml ammonium persulfate solution (in miliQ water) was added to the mixture for a final concentration of 18,24 mg/ml and magnetically stirred (750 rpm) at 40ºC for 17 hours, in order to start the polymerization reaction.

After 17 hours, the produced NPs followed various washing steps. The reaction mixture was centrifuged at 11000 rpm for 40 min at 4ºC with the supernatant retrieved and stored for drug-loading efficiency analysis in the case of KTG-loaded PEDOT NPs. MiliQ water was newly added, and the pellet was thoroughly resuspended by 5 min vortex and 15 min ultrasonication (Ultrasonic Cleaner; VWR). These centrifugation-resuspension cycles were repeated 2 more times, and after the final centrifugation, the supernatant was retrieved and the nanoparticles were dried in an oven for 3 days in order to completely remove the solvent.

2.2 Dynamic light scattering

The size and zeta potential of PEDOT and KTG-loaded NPs resuspended in miliQ water at 1 mg/ml were assessed trough dynamic light scattering (DLS) in a Zetasizer (Malvern Panalytical). The refractive index of the suspension was water, as in accordance with Bocca et.all[10].

2.3 Cyclic voltammetry

In order to study the electrochemical properties of the produced NPs, cyclic voltammetry (CV) was employed. A 5 mg/ml suspension of NPs was put in a screen-printed electrode (Metrohm DropSens), which was submerged in a de-aerated 0.05% Tween 20 (Sigma Aldrich) solution prepared in phosphate buffered saline (PBS, Sigma Aldrich). The setup was combined with a Bipotentiostat µStat 300 (Metrohm DropSens). The assay was performed with a potential range of -0.8V to 1V and a sensitivity of 1x10-4 A/V, with scan rates of 0.01; 0.02; 0.04; 0.08; 0.1; 0.2 and 0.3 V/s.

2.4 High performance liquid chromatography

The encapsulation efficiency (EE%) and drug loading (DL) of KTG in the produced PEDOT NPs was determined by analyzing the supernatant obtained after centrifuging the reaction mixture through reverse-phase high performance liquid chromatography(HPLC), using a Luna C-18 column (Phenomex). The mobile phase was acetonitrile(ACN):water with 0,01% TVA Fisher Scientific) 10:90–100:0 (v/v) during the first 13 min, followed with 10:90 (v/v) for 9 min. The flow rate of the samples was 1 ml/min and they were analyzed at a wavelength of 274nm. The concentration of the samples was calculated through a calibration curve, were samples sample with 1, 5, 10, 25 ,50, 100, 150, 400 ug/mL were analyzed, while also allowing to infer the retention time of drug. EE% and DL were calculated using the following formulas:

$$EE\% = \frac{Initial\ KTG\ mass\ -free\ KTG\ mass\ in\ supernatant}{Initial\ KTG\ mass}$$

$$DL = \frac{Initial\ KTG\ mass\ (mg) - free\ KTG\ in\ supernatant}{final\ nanoparticle\ mass}$$

The controlled release of KTG from KTG/PEDOT NPs with electrical stimulation was also assessed through HPLC. A PBS solution with 15 ug/mL of NPs and 0.003% Tween 20 was electrically stimulated for 3 x 3 min (30 second rest between each stimulation) between -3 and 3 V at a frequency of 500 mHZ using a AFG1022 potentiostat (TEKTRONIX) and a custom made 12-well plate lid with parallel titanium electrodes (0.8 cm apart). The solution was then retrieved and analyzed by HPLC as described previously.

2.5 Hydrogel fabrication

For the characterization assays, hydrogels were fabricated using HyStem® hydrogel kit (Advanced Biomatrix), following the manufacturer's instructions. Glycosil and Extralink were reconstituted with 1 and 0.5 ml of degassed water respectively, vortexed immediately, and placed on a rocker platform for 1 hour until the components were fully dissolved. This was followed by the production of three distinct hydrogel HyStem-CS; HyStem-CS-PEDOT:PSS; HyStem-CS-PEDOT NPs. For fabrication, glycosil was supplemented with CS (Sigma) to a final concentration of 1% v/v, and Clevios™ PH1000 PEDOT:PSS (Heraeus Epurio) or PEDOT NPs were added to a final concentration 10% v/v or 0.2 mg/ml, respectively were added. Finally, Extralink was added to the different glycosil mixtures in a 1:4 v/v ratio in order to start the cross-linking process.

The hydrogels to be used as scaffolds for human bone marrow-derived MSCs (hBMSCs) were prepared as previously described, but KTG/PEDOT NPs were added to a final concentration of 14 ug/ml prior to addition of the cross-linker.

2.6 Water content and swelling ratio

To assess water content (WC), the newly formed hydrogels were left in eppendorfs at RT for 7 days until they were completely dry. In the case of swelling ratio (Q), newly formed hydrogels were left at RT for 1 day, and then hydrated in excess PBS at RT. The weight of the hydrating hydrogels was measured at timed intervals, after excess water was removed by gentle blotting. Four (n=4) independent hydrogels were used in the analysis. The water content and swelling ratios were calculated as follows:

$$WC = \frac{Initial\ gel\ weight\ -Dry\ gel\ weight}{Initial\ gel} \times 100$$

$$Q = \frac{Hidrated\ gel\ weight\ (mg) - Initial\ gel\ weight\ (mg)}{Ininitial\ gel\ weight\ (mg)} \times 100$$

2.7. Rheology

The rheological properties of the produced hydrogels were assessed using an MCR 92 modular compact rheometer (Anton Paar). The measurement was made using a cone-plate geometry with a cone diameter of 50 mm, and a constant measurement gap of 0.1 mm, with a sample volume of 0.5 ml. The elastic behavior of the gels was studied through an oscillating time sweep test, were the time dependent storage modulus (G') and loss modulus (G'') were recorded, with a frequency of 1 Hz at 25ºC for 90 min. An amplitude sweep test was also performed at a frequency of 1 Hz at 25ºC until a maximum strain of 200% was reached.

2.8 Electrochemical impedance spectroscopy

The impedance of newly formed hydrogels was analyzed through electrochemical impedance spectroscopy (EIS) using a PalmSens4 potentiostate and the PSTrace5 software (PalmSens). The samples were put between 2 stainless steel cylindrical electrodes that measured the voltage. In order to maintain the contact area with the electrode's surfaces the same across the different gel samples, these were produced in identical 3D printed molds. To keep the distance between the electrodes across the

different sample measurements the same, a circular mold was put between the electrodes (without directly contacting them), that prevented them to come closer after contact with the hydrogel surfaces. The assay was performed at a fixed potential of 0.01 V, with a frequency range of 0.01 to 100000 Hz (n=1)

2.9 hBMSC culture

The human hBMSCs used in this thesis were part of the cell bank available at the Stem Cell Engineering Research Group, Institute for Bioengineering and Biosciences (iBB) at Instituto Superior Técnico. Vials with cryopreserved hBMSCs (Donor: Male 46 years) were thawed at 37ºC in a water bath. Afterwards, the cells were diluted in cell culture medium (1:6, v/v) - low glucose Dulbecco's Modified Eagle Medium (DMEM; Gibco Thermo Fisher Scientific) supplemented with 10% v/v fetal bovine serum (FBS; Gibco, Thermo Fisher Scientific) and 1% v/v antibiotic-antimycotic solution (Anti-Anti Solution; Gibco, Thermo Fisher Scientific) - and centrifuged for 7 minutes at 1250 rpm. Afterwards, the supernatant was removed, and the cells were resuspended in fresh culture medium, counted using the trypan blue (Trypan blue solution 0.4%; Gibco, Thermo Fisher Scientific) exclusion method, and plated on a T-flask at a cell density of 3000 cells/cm^2 that was kept at 37ºC and 5% CO2 in an incubator. Culture media was fully renewed every 3-4 days. Cell passaging was performed when hBMSCs reached 90% confluence. For that, cells were washed with PBS, incubated with a trypsin solution (0.05%, v/v) (Trypsin; Gibco, Thermo Fisher Scientific) for 7 minutes at 37ºC and 5% CO2 in order for the cells to detach, and afterwards centrifuged and counted. The cells were then distributed in the appropriate number of cell culture flasks at a density of 3000 cells/cm^2. All experimental assays were performed using hBMSCs between passage 3 and 5.

2.10 Assessment of the chondrogenic inducing potential of KTG/PEDOT NPs and HA-CS-KTG/PEDOT NPs hydrogels with and without electrical stimulation

To understand the effects of KTG-loaded nanoparticles in the chondrogenic differentiation of hBMSCs, 2.6x10^4 hBMSCs/cm^2 were seeded in a 12-well plate and supplemented with incomplete chondrogenic media - DMEM high glucose with 100nM dexamethasone (Sigma-Aldrich), 50 ug/ml ascorbic acid (Sigma-Aldrich), 40 ug/ml L-proline (Sigma-Aldrich), 1% v/v ITS + supplement (Corning), 1 mM sodium pyruvate and 1% v/v Anti-Anti solution – supplemented with 2 ug/ml of KTG/PEDOT NPs or PEDOT NPs. It is important to note the absence of TGF-B3 in the media composition. The differentiation was carried through 21 days, with media being exchanged every 3 to 4 days. With every media exchange, the wells were thoroughly washed with PBS to retrieve the remaining NPs, and new NPs at 2 ug/mL were added. With each exchange, the cells were electrically stimulated for 3 x 3 min (30 second rest between each stimulation) between -3 and 3 V at a frequency of 500 mHZ. Cells seeded in the absence of NPs and non-stimulated correspondent groups were used as controls. In the case of the hydrogels, the assay was performed similarly, where 2.22x10^5 hBMSCs/mL hydrogel were encapsulated in a HA-CS hydrogel together with 14 ug/mL KTG/PEDOT NPs or PEDOT NPs, but no new NPs were added with each media exchange. hBMSCs encapsulated in HA-CS hydrogel and non-stimulated correspondent groups were used as controls.

2.11 Cell viability and metabolic activity assays

The metabolic activity of hBMSCs (2D cultures in plates or 3D hydrogel cultures) was measured on days 3, 7, 14 and 21 of the culture using the Alamar Blue assay as previously described (n=3). To account for possible hydrogel autofluorescence, acellular hydrogels were used as blank controls. For the case of hydrogels, cell viability was confrimed after 21 days of culture through a LIVE/DEAD assay as previously described, and observed under fluorescence microscopy.

2.12 Sulfated GAGs quantification

After 21 days of culture the cells in 2D cultures were harvested, centrifuged, and the obtained cell pellets were frozen and stored at -80ºC until further use.. In the case of the hydrogels, these were digested with 40 mM N-acetyl cysteine and the cells were collected and centrifuged, which yielded a cell pellet with some hydrogel.remainants.

The measurement of sulfated GAG levels was made using a 1,9-Dimethylmethylene Blue (DMMB, Sigma-Aldrich) assay. A DMMB dilution buffer pH 6.5 (50 mM sodium phosphate (Sigma-Aldrich), 2 mM N-acetyl cysteine (Sigma-Aldrich) and 2 mM EDTA (Merck) in ultrapure miliQ water) was prepared. DMMB stock solution pH 3 was prepared by adding a 3.2 mg/mL DMMB in absolute EtOH solution (Sigma-Aldrich) to a solution of 2.73 g NaCL and 3.04 gL glycine in ultrapure MiliQ water, with a total volume of 1L. The previously obtained pellets were digested with a 0.1 mg/mL papain (from papaya latex, Sigma-

Aldrich) in DMMB dilution buffer solution for 16 hours at 60ºC. Afterwards, DMMB stock solution was mixed with the digested pellets in 96-well plates. The mixtures were incubated for 5 min at RT, and the fluorescence was read at 525 nm in a plate reader (n=1). The amounts of sGAG for each condition were calculated by recurring to a calibration curve using chondroitin sulfate (sodium salt from bovine cartilage, Sigma-Aldrich) standards. The GAG amounts were then normalized to the metabolic activity of the cells at day 21 of differentiation.

3. Results and discussion

3.1 Nanoparticle size and stability

The size of the PEDOT and KTG-loaded PEDOT NPs was determined through DLS, with effective diameters of 99 ± 71 and 172 ± 90 nm respectively. The size distribution of the particles is represented by the polydispersity index (PdI), which ranges from 0 to 1, with 0 being a homogenous nanoparticle population and the latter being a highly heterogeneous one. Despite both being somewhat heterogeneous, PEDOT NPs (PdI = 0.245) were significantly less heterogeneous than the KTG-loaded NPs (PdI = 0.490), which can also be seen through the lower size standard deviation. The dispersity among the NP populations can be explained by the lack of full control during the synthesis process, and the chemical reactions during NP development not being homogenous processes, which often introduces intra and inter-batch heterogeneities[11]. In fact, this might explain the higher PdI of KTG-loaded PEDOT NPs, as the introduction of an additional molecule to the formulation (when compared to PEDOT NPs) introduces further complexity to the chemical synthesis, elevating heterogenies.

DLS was also utilized to measure the ζ-potential of the NPs, which came at -71 mV for PEDOT and -75 mV for KTG-loaded NPs. The ζ-potential can give insight on the stability and eletrokinetic potential of an NP colloidal dispersion, being the potential difference between the dispersion medium and the stationary layer surrounding the NP. Because the particle surface has a charge, it creates a surrounding bound layer with the correspondent counter-ions, traveling with the nanoparticle as it diffuses through the dispersion. Hence, the magnitude of the ζ-potential indicates the degree of electrostatic repulsion between particles with the same charge, were higher values (either positive or negative) indicate a higher repulsion, and thus a resistance to NP aggregation and flocculation. The produced NPs have absolute ζ-potentials above 61 mv, which is the threshold were particles are considered highly stable. In fact, these nanosuspensions were able to maintain stability for over 2 months without significant sedimentation due to particle aggregation.

3.2 Electrochemical properties

The electrochemical response of the produced nanoparticles, adsorbed to the electrode surface, was assessed through CV, which registered oxidation-reduction cycles within a potential range of -0.8 and 1 V at different scan rates (figure 1). PEDOT NPs demonstrated a typical anodic peak at around 0 V, and a cathodic peak at around -0.2V which is close to what has been previously describe[12]. As kartogenin is a compound that also experiences redox behavior, the KTG/PEDOT NPs voltammograms can get partially "masked" by KTG. This is evident by the appearance of a "shoulder" to the right of the previously mentioned oxidation peak at 0 V, meaning the drug has an irreversible oxidation peak at 0.2 – 0.3 V, depending on the scan rate. However, another irreversible oxidation peak at 0.6-0.7 V, depending on the scan rate, can also be observed. Overall, these results confirmed that the produced PEDOT and KTG/PEDOT NPs are electroactivity, which will allow the use of electro stimulation to trigger the release of the drug.

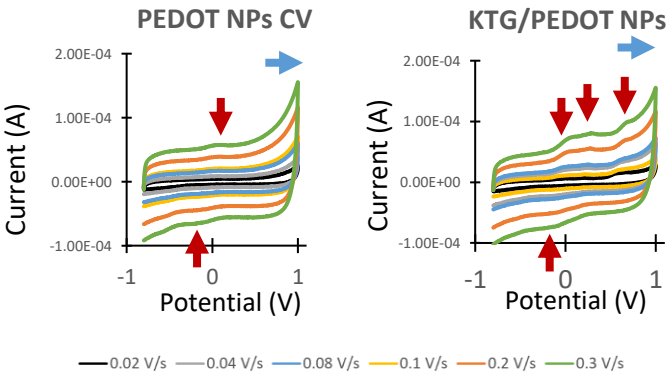

Figure 1 – Voltammograms of PEDOT and KTG/PEDOT nanoparticles obtained by cyclic voltammetry. The voltage range was -0.8 to 1 V, and the assay was performed at various scan rates (0.02, 0.04, 0.08, 0.1, 0.2 and 0.3 V/s) for both nanoparticle formulations (n=2). Red arrows point to oxidation and reduction peaks, and blue arrow to the direction of the scan.

3.3 Controlled KTG release with electrical stimulation

In order to assess if the release of KTG could be controlled though electrical stimulation, 15 ug/mL KTG/PEDOT NPs in PBS with 0.003% Tween 20 were stimulated once or twice with an alternating current, with potentials being cycled between -3 and 3

V at a frequency of 500 mHz for 3 min. In figure 2 the HPLC chromatograms of the media can be observed. It is possible to see that the KTG/PEDOT sample that received no stimulation didn't exhibit drug release, evidenced by the lack of a peak at a retention time of 10.67, correspondent to the KTG retention time. However, the sample that was stimulated once showed a peak at the KTG retention time with an area of 24 mAU.s, with the same peak having an area of 49 mAU.s in the samples that were stimulated twice. Through a prepared calibration curve, it was estimated that there was a 5 and 10.5% KTG release from NPs stimulated once or twice respectively in these conditions. This result indicates that KTG can be controllably released from KTG/PEDOT NPs with electrical stimulation without significant passive release.

The proposed release mechanism of the drug is a combination of changes in the electrostatic interaction between the drug and conductive polymer and an actuation response of the latter. By cycling through voltages, the electroactive PEDOT NPs and the loaded drug will experience oxidation/reduction cycles. In an oxidation cycle, both polymer and drug will become oxidated, increasing the positive charge within the NPs. This will create repulsive interactions between the two species, driving the release of the drug[13,14]. This effect is further amplified by PEDOT actuation. When reducing PEDOT NPs, electrons are injected into the polymer chains, compensating the positive charges acquired in the oxidation cycle. To maintain overall electroneutrality, negatively charged counterions are expelled to the media, inducing the contraction of the particles[15]. This event produces a hydrodynamic pressure inside the particle that causes expulsion of the drug. Furthermore, actuation creates cracks and holes in the polymer, that can aid the release of the drug[16]. As such, by using alternating current, oxidation and reduction cycles can be applied to the nanoparticles, altering electrostatic interactions, and producing cycles of actuation that cause frequency dependent contractions and cracks.

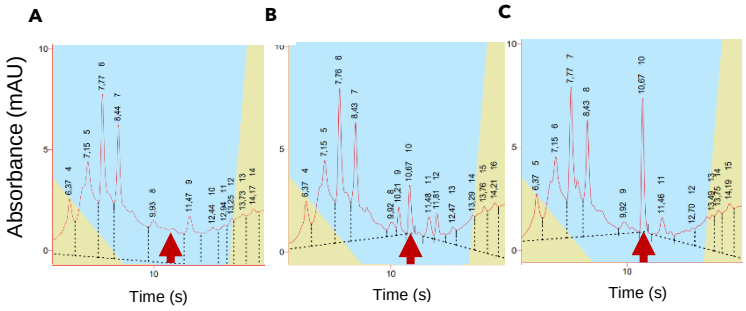

Figure 2 – HPLC chromatograms of (A) un-stimulated KTG/PEDOT NPs, (B) KTG/PEDOT NPs stimulated 1 time with the referred stimulation protocol and (C) KTG/PEDOT NPs stimulated 2 times. Red arrows point to the retention time of KTG (n=1).

3.4 Water content and swelling ratio

As articular cartilage is heavily encompassed by water, one of the crucial properties of hydrogels would be their high water content, which is critical to support integrity and diffusion of substances[17]. Furthermore, besides the innate amount of water they carry upon fabrication, the capacity of the scaffold to absorb surrounding water is also an important property, as it can have a profound impact on its mechanical properties[18]. The water content of three types of hydrogels (HA-CS; HA-CS-PEDOT:PSS and HA-CS-PEDOT NPs) was calculated by subtracting the weight of completely dry scaffolds to the wet weight post-fabrication. Every hydrogel formulation exhibited a very similar high water contents, of around 97%. To assess swelling ratio, newly formed hydrogels were left incubating at RT in order for the unbound superficial water to evaporate. They were afterwards immersed in excess PBS and their weight was followed for 7 days (figure 3). Significant differences between the different hydrogel formulations were observed. HA-CS hydrogels exhibited a constant increase in swelling ratio for the first 108 h, followed by no significant changes in swelling. Both HA-CS-PEDOT:PSS and HA-CS-PEDOT NPs hydrogels showed limited swelling, with a maximum of 13.87% for the former and 6.04% for the latter. Interestingly, in the first 40 hours, the swelling rates of both formulations appeared near identical. One of the reasons for a lower water absorption among these formulations could be the apparent lower porosity observed through SEM[19]. Introduction of PEDOT:PSS and PEDOT NPs could act as cross-linking points for the polymer, resulting in stronger interactions between polymer chains, tightening the gel structure and creating stiffer scafolds[20]. Consequently, the mobility of polymers chains is hindered, minimizing water absorption. Lower swelling rates in hydrogels with embedded nanoparticles have been observed in other studies[21,22]. As articular cartilage is a water rich tissue, swelling-resistant hydrogels for CTE applications are invaluable. This property allows hydrogels to be injected into a damage site, without absorbing the surrounding body fluid, preserving its mechanical properties, and not damaging surrounding tissues[23].

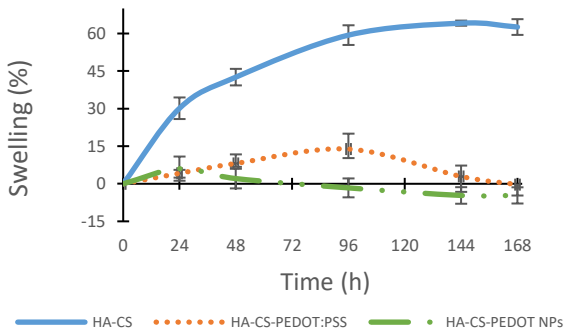

Figure 3 – Swelling rate of HA-CS, HA-CS-PEDOT:PSS and HA-CS-PEDOT NPs over the course of 7 days. Error bars for each measurement are represented (n=4).

3.5 Hydrogels gelation kinetics

In order to analyze the gelation kinetics of the hydrogels, an oscillating time sweep assay was performed. The different formulations of hydrogels were prepared, and, after addition of the cross-linker, the assay was swiftly initiated, with the storage and loss modulus being recorded (figure 4). Since hydrogels are initially aqueous flowable solutions, it is expected G'' to be, initially higher than G', as the hydrogel will mainly act as a viscous liquid. However, when cross-linking occurs and the hydrogel experiences a sol-gel transition, the material should exhibit a more elastic response, with G' > G''. As such, the crossover of G' and G'' splits the hydrogel gelation process in two stages, primarily viscous when G' < G'' and primarily elastic when G' > G'', being a measure of gelation time141. For the HA-CS hydrogel, it can be observed that the crossover time was right in the beginning of the measurement, meaning gelation started occurring as soon as the cross-linker was added. However, this was unexpected, as the producers of the Hystem hydrogel kit state gelation occurs after 20 min. This could be both due to differences in definitions of gelation time, as the producers don't state the method used for this determination (many times a visual tube inversion test is used to infer gelation[25]), or due to the addition of CS to the formulation. Despite a different hydrogel formulation and experimental setup, another work measuring gelation of a HA-CS hydrogel through a rheological time-sweep also reported an instant gelation after addition of the cross-linker[26]. In the case of HA-CS-PEDOT NPs, an initial viscous response can be observed after the addition of the cross-linker until crossover at 22.5 min. It appears that the cross-linking in this hydrogel had a slight delay, starting a very low G' value that had a sudden increase at 8 min. For HA-CS-PEDOT NPs hydrogel, a definite crossover can be detected at 29 min, although it is difficult to claim a definite gelation time due to high fluctuations of G' and G'' for the first 18 min. These fluctuations are likely caused by a setup error, as G' will be dependent on the cross-linking state of the hydrogel, which is irreversible[27] and thus should not fluctuate. Overall, both PEDOT:PSS and PEDOT NPs hydrogels exhibited gelation times close to the Hystem kit fabricator's stated time at, 22.5 and 29 min respectively. The longer gelation times can actually be beneficial or even crucial for CTE strategies employing injectable hydrogels, as the scaffolds can more easily fit surgical requirements by staying in a sol state for a longer period of time after addition of the crosslinker. In this sol state, hydrogels can be more easily manipulated and injected to a damaged cartilage site, having enough time to match the defect and only then transition to a gel phase and start adhering.

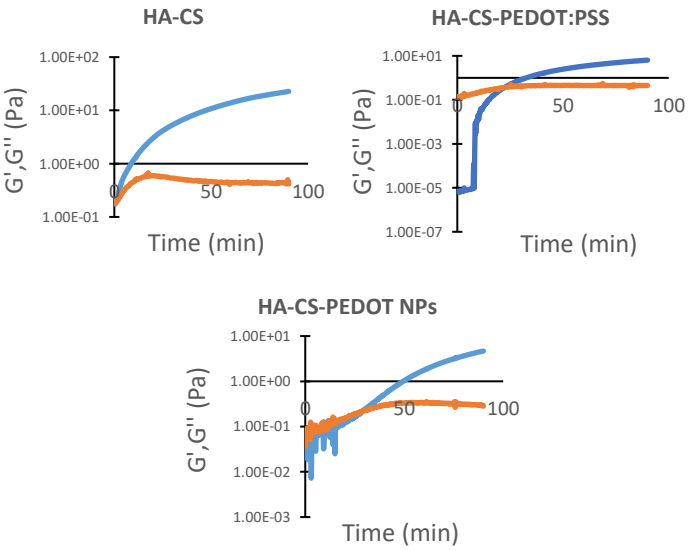

Figure 4 – Oscillating time sweep showing the gelation kinetics through storage (G') and loss modulus (G'') of HA-CS, HA-CS-PEDOT:PSS and HA-CS-PEDOT NPs. G' and G'' crossover indicates gelation (n=1).

For this work, the impedance of the hydrogels is a key parameter, as it is important not only for the correct mimicking of the native tissue electrochemical properties, but also for the effective trigger of drug release through electrical stimulation. Conductive hydrogels can allow a more effective transmission of electric signals to the seeded cells and the embedded nanoparticles without the use of high potentials[28]. frequency dependent impedance of the 3 hydrogel formulations was measured through electrochemical

impedance spectroscopy (figure 5). In This technique, a sinusoidal potential is applied to an electrochemical system (in this case the various hydrogels) and measures the sinusoidal potential out of the system. The frequency dependent impedance (Z) is given by the ratio between the applied voltage and the measured current. From the impedance curves, it is possible to observe that all hydrogels exhibited low impedance, at high frequency values. However, at lower frequencies, like the ones found in electroactive tissues (1Hz)[29], resistive currents dominate, with higher impedances for all hydrogel formulations being observed. However, it is clearly visible that the addition of PEDOT:PSS or PEDOT NPs notably decreasea the impedance of the hydrogels across the entire frequency range. Various other works have highlighted the potential to modulate hydrogel conductivity with the addition of conductive polymers[30–33]. The dependence of hydrogel conductivity with the present of PEDOT:PSS or nanoparticles presents a powerful tool to fine-tune the electrical properties of the scaffolds for cartilage regeneration. For the system of this particular work, the concentration of KTG/PEDOT embedded in the hydrogels, to serve as scaffolds for hBMSCs, can be modified in order to confer different degrees of conductivity. This effect might be crucial and important to optimize in order to ensure that the applied electrical stimulation is enough to trigger the release of KTG from the nanoparticles.

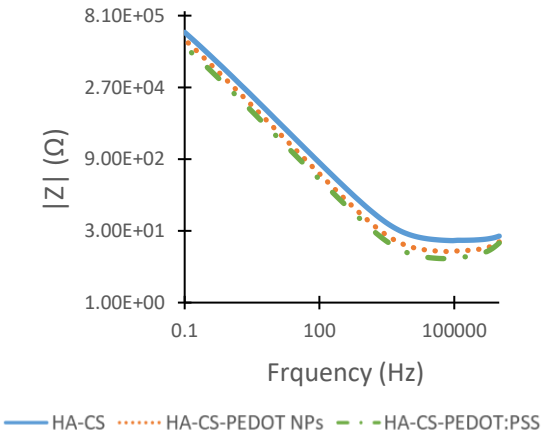

Figure 5 – Electrochemical impedance spectroscopy results of HA-CS (control), HA-CS-PEDOT:PSS (PSS) and HA-CS-PEDOT NPs (NPs) with frequency-variable impedance.

3.6 Assessment of the chondrogenic inducing potential of KTG/PEDOT NPs and HA-CS-KTG/PEDOT NPs hydrogels with electrical stimulation

In order to study the potential of the designed system to regenerate articular cartilage, its effects on the proliferation and chondrogenic differentiation of MSCs either in a 2D environment or embedded in NP embedded hydrogels was assessed. As a prominent component of native articular cartilage, sGAG production was used to quantify chondrogenic differentiation. Figure 6 shows the GAG production of MSCs cultured for 21 days in a 2D environment with incomplete chondrogenic media without NPs or supplemented with PEDOT or KTG/PEDOT NPs. It is possible to see that all in all the conditions (except KTG/PEDOT NPs with electrical stimulation) the near same amount of GAGs was present, which translates to a similar level of chondrogenic differentiation. The close amount of GAG levels between electrically stimulated or un-stimulated samples (control and PEDOT NPs) indicates that the stimulation did not have direct effects on hBMSCs chondrogenesis. However, in the case of KTG/PEDOT NPs, the samples that received electrical stimulation exhibited a significant increase of GAG levels when compared to unstimulated samples. Despite this particular electrical stimulation protocol not showing direct effects on cell chondrogenesis, it is capable to trigger the release of KTG loaded in the NPs. These results not only further confirm the controllable drug release, but also show the effectiveness of KTG in inducing the chondrogenesis of hBMSCs.

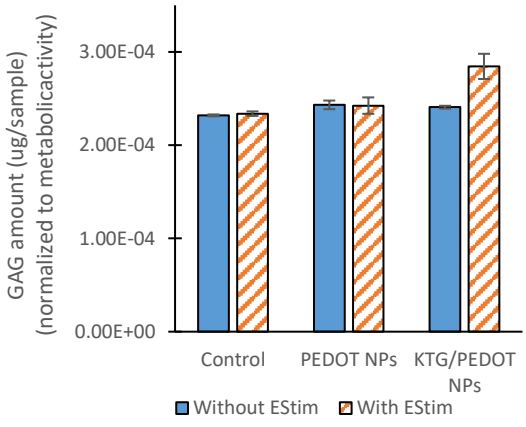

Figure 6 – Sulfateds GAG content of each sample after 21 days of chondrogenic differentiation. GAG levels were normalized to the metabolic activity of hBMSCs on day 21 of the assay (n=1).

MSCs were also embedded in NP embedded hydrogels, and cultured in incomplete chondrogenic media for 21 days, being either electrically stimulated

or unstimulated. The metabolic activity fold increase between day 21 and 3 can be seen on figure 7. Interestingly, the fold increase of HA-CS-PEDOT and HA-CS-KTG/PEDOT NPs was significantly higher than the HA-CS hydrogels, both with and without electrical stimulation, meaning the embedded hBMSCs exhibited higher proliferation rates in the scaffolds formulated with NPs. This difference is likely caused by changes in the hydrogel's physical properties introduced by the NPs. As previously discussed, the introduction of nanoparticles to the formulations likely caused denser hydrogel cross-linking, which in turn generates stiffer scaffolds. Hydrogels stiffness plays a key role in cell-matrix interactions and cell behavior[34]. In fact, MSCs have demonstrated increased proliferative potential when cultured on stiff hydrogels compared with softer hydrogels[35] which corroborates the obtained results. The dependence of hBMSC proliferation on the mechanical properties of the scaffold is something that can be explored in future assays by modulating the concentration of NPs in the hydrogel formulation. Besides the differences in hBMSC proliferation observed between plain and NP embedded hydrogels, interesting results can also be observed between samples with or without electrical stimulation. In the case of HA-CS and HA-CS-PEDOT NPs hydrogels, no significant changes can be observed between stimulated and non-stimulated samples. However, in the case of HA-CS-KTG/PEDOT NPs hydrogels, samples that were electrically stimulated exhibited a significantly higher fold increase when compared to unstimulated samples. This indicates that electrical stimulation triggered a response in these hydrogels that led to an increase in the proliferation rate of hBMCSs, which was likely the release of KTG from the gel-embedded NPs, triggered by the stimulation. KTG has been seen to increase the metabolic activity of chondrocytes and adipose-derived stem cells elsewhere, although the mechanism that led to this increase remained unclear[36,37]. However, a possible explanation could be that KTG activates RUNX1, a transcription that plays important role in the differentiation in chondrocyte proliferation[38]. The similar fold increase observed between non-stimulated HA-CS-KTG/PEDOT and HA-CS-PEDOT NPs hydrogels further corroborates the involvement of KTG release in the increase of hBMSC proliferation rate. As It was previously seen, the passive release of KTG from KTG/PEDOT NPs is almost null, meaning that in the absence of electrical stimulation to trigger its release, similar results should be expected between drug-loaded and unloaded PEDOT NPs.

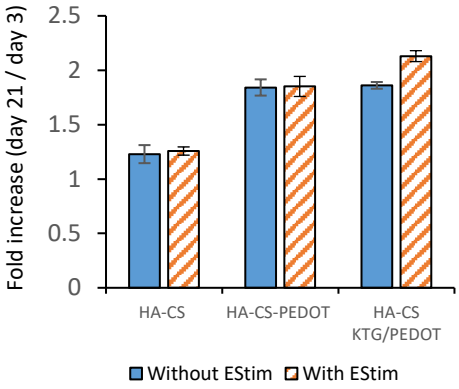

Figure 7 – Fold increase of the metabolic activity of hBMSCs embedded in HA-CS, HA-CS-PEDOT and HA-CS-KTG/PEDOT NPs between days 21 and 3 (n=3).

4. Conclusion

This MSs thesis focused on developing a novel system for cartilage regeneration by employing principles of CTE, aiming to construct scaffolds that could act as substitutes for native cartilage and promote its regeneration. As such, hydrogels were as scaffolds for hBMSCs and a drug delivery system that allowed the controlled delivery of KTG through electrical stimulation, promoting the chondrogenesis of embedded cells. In this work, KTG was successfully loaded in PEDOT NPs with a high efficiency, and its encapsulation was confirmed through various assays. Through cyclic voltammetry, the produced NPs were seen to be electroactive, which allowed for a controlled release of encapsulated KTG through electrical stimulation. As chondrogenic differentiation is a 21-day process, the drug delivery system presented in this work may be optimal for effectively promoting differentiation, allowing a stimuli dependent delivery of controllable doses along the entire differentiation process. However, further assays regarding KTG release triggered by electrical stimulation need to be conducted.

The addition of NPs to HA-CS hydrogels significantly lowered the swelling ratio of the scaffolds without compromising their water content, which would allow them to retain their mechanical strength in an in vivo environment. Additionally, this addition also enhanced the conductivity and mechanical strength of the scaffolds. The results obtained highlight the customization potential of this hydrogel, were adjusting NP concentration allows the modulation of crucial properties required to create a scaffold that mimics native cartilage. Furthermore, as the addition of NPs prolonged the gelation time of the hydrogels,

these could potentially be utilized as injectable hydrogels, which would further aid their clinical translation.

hBMSCs cultured with KTG/PEDOT NPs exhibited higher levels of GAGs when electrically stimulated, pointing to an effective release of the drug that promoted the chondrogenic differentiation of the cells. In hydrogels fabricated with NPs, embedded hBMSCs exhibited enhanced proliferation, which was likely a caused by the increased stiffness of the scaffold. Interestingly, cells embedded in HA-CS-KTG/PEDOT NPs hydrogels that were electrically stimulated showed increased proliferation, suggesting the release of KTG from the nanoparticles. Despite the promising results regarding the effectiveness of the system in promoting the proliferation and chondrogenic differentiation of MSCs, further assays are required in order to draw definitive conclusions.

5. Future perspectives

The development of a CTE inspired system capable of mimicking the properties of native cartilage, and allow a controlled drug delivery, is a very promising approach to target cartilage regeneration. If correctly optimized, this system has the potential for an effective clinical translation, where the NP embedded hydrogels could be injected into damaged cartilage sites of patients, and already existing devices could be used to electrically stimulate the tissue, triggering the KTG release and promoting regeneration. However, the is still a need for further investigation and optimization in order to make this a reality.

In the future, some of the assays performed for this work need to be re-conducted, in order to gather more robust results. The KTG release assays should be re-done in triplicates, and more electrical stimulation conditions studied, possibly by changing stimulation times and frequencies. KTG release assays should also be performed with NP embedded hydrogels, as the conduciveness of the hydrogel can influence the effectiveness of electrical stimulation on drug release. The quantification of GAGs and gene expression analysis also require further analysis to acquire more robust results.

After confirming the results obtained for this work with future assays, the hydrogels and stimulation protocol need to be optimized in order to not only construct a native cartilage mimetic scaffold, but to maximize tissue regeneration potential through cell proliferation and differentiation. In order to achieve this, the hydrogel's composition should be adjusted, by changing crosslinker and nanoparticle concentrations, with posterior rheological characterizations. Furthermore, as a key parameter for an effective clinical translation, the biodegradability of the hydrogels needs to be improved, possibly by introducing biodegradable materials to their formulation. In terms of electrical stimulation, a deeper dive in the molecular mechanisms behind the chondrogenic inducing abilities of KTG should be taken, as drug delivery timings could improve the chondrogenic differentiation of MSCs.

6. References

1. Woo, S. L. & Buckwalter, J. A. Injury and repair of the musculoskeletal soft tissues. Savannah, Georgia, June 18–20, 1987. *Journal of Orthopaedic Research* **6**, 907–931 (1988).
2. Sophia Fox, A. J., Bedi, A. & Rodeo, S. A. The Basic Science of Articular Cartilage: Structure, Composition, and Function. *Sports Health* **1**, 461 (2009).
3. Goldring, S. R., Goldring, M. B. & Goldring, S. R. Clinical aspects, pathology and pathophysiology of osteoarthritis. *J Musculoskelet Neuronal Interact* **6**, 376–378 (2006).
4. Zhang, Y. & Jordan, J. M. Epidemiology of Osteoarthritis. *Clin Geriatr Med* **26**, 355 (2010).
5. Plotnikoff, R. *et al.* Osteoarthritis prevalence and modifiable factors: A population study Chronic Disease epidemiology. *BMC Public Health* **15**, 1–10 (2015).
6. Gu, Y.-Y. *et al.* Research progress on osteoarthritis treatment mechanisms. *Biomedicine et Pharmacotherapy* **93**, 1246–1252 (2017).
7. Turkiewicz Y Z *, A. *et al.* Current and future impact of osteoarthritis on health care: a population-based study with projections to year 2032. *Osteoarthritis Cartilage* **22**, 1826–1832 (2014).
8. Daher, R. J., Chahine, N. O., Greenberg, A. S., Sgaglione, N. A. & Grande, D. A. New methods to diagnose and treat cartilage degeneration. *Nature Reviews Rheumatology 2009 5:11* **5**, 599–607 (2009).
9. Tuli, R., Li, W. J. & Tuan, R. S. Current state of cartilage tissue engineering. *Arthritis Res Ther* **5**, 235–238 (2003).
10. Bocca, B., Sabbioni, E., Mičetić, I., … A. A.-J. of A. & 2017, undefined. Size and metal composition characterization of nano- and microparticles in tattoo inks by a combination of analytical techniques. *J. Anal. At. Spectrom* **32**, 616–628 (2017).
11. Stavis, S. M., Fagan, J. A., Stopa, M. & Liddle, J. A. Nanoparticle Manufacturing-Heterogeneity through Processes to Products. *ACS Appl Nano Mater* **1**, 4358–4385 (2018).
12. Dietrich, M., Heinze, J., Heywang, G. & Jonas, F. Electrochemical and spectroscopic characterization of polyalkylenedioxythiophenes. *Journal of Electroanalytical Chemistry* **369**, 87–92 (1994).
13. Miller, L. L., Zhou, X. Q., Miller, L. L. & Zhou, X. Q. Poly(N-methylpyrrolylium) poly(styrenesulfonate) - a conductive, electrically switchable cation exchanger that cathodically binds and anodically releases dopamine. *MaMol* **20**, 1594–1597 (1987).
14. Bidan, G., Lopez, C., Mendes-Viegas, F., Vieil, E. & Gadelle, A. Incorporation of sulphonated cyclodextrins into polypyrrole: an approach for the electro-controlled delivering of neutral drugs. *Biosens Bioelectron* **10**, 219–229 (1995).
15. Gandhi, M., Murray, P., Spinks, G., metals, G. W.-S. & 1995, undefined. Mechanism of electromechanical actuation in polypyrrole. *Synth Met* **73**, 247–256 (1995).
16. Abidian, M. R., Kim, D. H. & Martin, D. C. Conducting-Polymer Nanotubes for Controlled Drug Release. *Adv Mater* **18**, 405 (2006).
17. Gun'ko, V. M., Savina, I. N. & Mikhalovsky, S. v. Properties of Water Bound in Hydrogels. *Gels* **3**, 37 (2017).
18. Kamata, H., Akagi, Y., Kayasuga-Kariya, Y., Chung, U. il & Sakai, T. 'Nonswellable' hydrogel without mechanical hysteresis. *Science (1979)* **343**, 873–875 (2014).
19. Yacob, N. & Hashim, K. Morphological effect on swelling behaviour of hydrogel. **1584**, 153 (2014).
20. Mulhbacher, J., Ispas-Szabo, P. & Mateescu, M. A. Cross-linked high amylose starch derivatives for drug release: II. Swelling properties and mechanistic study. *Int J Pharm* **278**, 231–238 (2004).
21. Lee, W. F. & Tsao, K. T. Effect of silver nanoparticles content on the various properties of nanocomposite hydrogels by in situ polymerization. *J Mater Sci* **45**, 89–97 (2010).

22. Paydayesh, A., Heleil, L. & Dadkhah, A. S. Preparation and application of poly (hydroxyl ethyl methacrylate) nanocomposite hydrogels containing iron oxide nanoparticles as wound dressing. *Original Research Article Polymers and Polymer Composites* **30**, 1–10 (2019).
23. Mulder, M., Crosier, J. & Dunn, R. Cauda equina compression by hydrogel dural sealant after a laminotomy and discectomy: case report. *Spine (Phila Pa 1976)* **34**, 144–148 (2009).
24. Sun Han Chang, R., Lee, J. C. W., Pedron, S., Harley, B. A. C. & Rogers, S. A. Rheological Analysis of the Gelation Kinetics of an Enzyme Cross-linked PEG Hydrogel. *Biomacromolecules* **20**, 2198–2206 (2019).
25. Huynh, C. T., Liu, F., Cheng, Y., Coughlin, K. A. & Alsberg, E. Thiol-Epoxy 'click' Chemistry to Engineer Cytocompatible PEG-Based Hydrogel for siRNA-Mediated Osteogenesis of hMSCs. *ACS Appl Mater Interfaces* **10**, 25936–25942 (2018).
26. Mihajlovic, M. *et al.* Viscoelastic Chondroitin Sulfate and Hyaluronic Acid Double-Network Hydrogels with Reversible Cross-Links. *Biomacromolecules* **23**, 1350–1365 (2022).
27. Parhi, R. Cross-Linked Hydrogel for Pharmaceutical Applications: A Review. *Adv Pharm Bull* **7**, 515 (2017).
28. Yang, J., Choe, G., Yang, S., Jo, H. & Young Lee, J. Polypyrrole-incorporated conductive hyaluronic acid hydrogels. *Biomater Res* **20**, 31 (2016).
29. Spencer, A. R. *et al.* Electroconductive Gelatin Methacryloyl-PEDOT:PSS Composite Hydrogels: Design, Synthesis, and Properties. *ACS Biomater Sci Eng* **4**, 1558–1567 (2018).
30. Yang, J., Choe, G., Yang, S., Jo, H. & Young Lee, J. Polypyrrole-incorporated conductive hyaluronic acid hydrogels. (2016) doi:10.1186/s40824-016-0078-y.
31. Mihic, A. *et al.* A conductive polymer hydrogel supports cell electrical signaling and improves cardiac function after implantation into myocardial infarct. *Circulation* **132**, 772–784 (2015).
32. Pinelli, F., Magagnin, L. & Rossi, F. Can nanostructures improve hydrogel-based biosensors performance? *Nanomedicine* **16**, 681–683 (2021).
33. Phuchaduek, W., Jamnongkan, T., Rattanasak, U., Boonsang, S. & Kaewpirom, S. Improvement in physical and electrical properties of poly(vinyl alcohol) hydrogel conductive polymer composites. *J Appl Polym Sci* **132**, 42234 (2015).
34. Ahearne, M. Introduction to cell–hydrogel mechanosensing. *Interface Focus* **4**, 20130038 (2014).
35. Marklein, R. A. & Burdick, J. A. Spatially controlled hydrogel mechanics to modulate stem cell interactions. *Soft Matter* **6**, 136–143 (2009).
36. Baharlou Houreh, A., Masaeli, E. & Nasr-Esfahani, M. H. Chitosan/polycaprolactone multilayer hydrogel: A sustained Kartogenin delivery model for cartilage regeneration. *Int J Biol Macromol* **177**, 589–600 (2021).
37. Zhu, Y. *et al.* Development of kartogenin-conjugated chitosan–hyaluronic acid hydrogel for nucleus pulposus regeneration. *Biomater Sci* **5**, 784–791 (2017).
38. Wang, Y. J. *et al.* Runx1/AML1/Cbfa2 mediates onset of mesenchymal cell differentiation toward chondrogenesis. *Journal of Bone and Mineral Research* **20**, 1624–1636 (2005).